

## Consecutive Peierls distortions and high-pressure phase transitions in $\text{YH}_3$

Yansun Yao and Dennis D. Klug

*Steacie Institute for Molecular Sciences, National Research Council of Canada, Ottawa, Canada K1A 0R6*

(Received 13 November 2009; revised manuscript received 16 February 2010; published 12 April 2010)

High-pressure phase transformations in  $\text{YH}_3$  were investigated using the evolutionary algorithm for structural searches. A series of phase transformations are predicted with three lowest enthalpy phases identified. Two consecutive Peierls distortions within the hcp and fcc cells result into two low-pressure structures, the previously identified  $P\bar{3}c1$  structure and a predicted  $C2/m$  structure. The  $P\bar{3}c1$  structure transforms to a  $C2/m$  structure at 12 GPa and stabilizes to a fcc structure at 38 GPa. The predicted properties of the  $C2/m$  structure agree well with experimental observation. At 200 GPa, the fcc structure transforms to a hcp structure. At 214 GPa, a transformation analogous to a Burgers deformation becomes more favored in the hcp form and this results in a stable  $Cmcm$  structure.

DOI: [10.1103/PhysRevB.81.140104](https://doi.org/10.1103/PhysRevB.81.140104)

PACS number(s): 61.50.Ks, 71.20.Eh, 71.30.+h, 74.25.Jb

Yttrium can absorb hydrogen to form  $\text{YH}_x$  hydrides at ambient pressure. Upon H loading,  $\text{YH}_x$  hydrides undergo a reversible metal-insulator transition once  $x$  is increased close to 3.<sup>1</sup> After the transition, the hydrides become insulating and transparent. The transition occurs at room temperature and in the visible spectrum range, and therefore, it has led to potential applications of  $\text{YH}_x$  hydrides as switchable mirrors.<sup>1</sup> The electronic properties of  $\text{YH}_x$  hydrides can also be significantly modified by pressurization as well as hydrogenation. The insulating state of  $\text{YH}_3$  at ambient pressure will transform to a metallic phase if the pressure is sufficient. Upon compression, the ionicity of  $\text{YH}_3$  is decreased and a significant amount of electronic charge is transferred back to Y atoms. A series of studies have characterized the high-pressure phase transitions for  $\text{YH}_3$  up to 40 GPa.<sup>2–8</sup> At ambient pressure,  $\text{YH}_3$  forms a distorted hcp form identified with space group  $P\bar{3}c1$  by neutron diffraction.<sup>9–11</sup> There are two other suggested possible structures<sup>12,13</sup> that are almost energetically degenerate but not in agreement with recent neutron-diffraction data.<sup>14,15</sup> The ambient-pressure structure is shown to transform to the fcc structure over a large pressure span ranging from about 9 to 24 GPa.<sup>4–8</sup> There are experimental evidences showing an intermediate phase in this transition but the precise characterization of this structure is under debate.<sup>4,7</sup> During the phase transition, the band gap in  $\text{YH}_3$  starts to narrow in the intermediate phase and closes once the structure completely transforms into fcc. The pressure of metallization for  $\text{YH}_3$  is the lowest observed pressure for metallization of hydrogen-rich compounds to date. This suggests that high-pressure  $\text{YH}_3$  could be a promising candidate for metallization of hydrogen, as well as a good superconductor.<sup>16</sup> In this Rapid Communication, predictions of several high-pressure structures of  $\text{YH}_3$  are made, along with a characterization of their properties and mechanisms underlining the phase transitions, in an effort to explain the distinct properties of  $\text{YH}_3$  at different pressures. In particular, we provide more detailed structural characterizations in addressing the intermediate phase between  $P\bar{3}c1$  and fcc structures. Moreover, since structural data for  $\text{YH}_3$  so far are only reported up to 40 GPa,<sup>6,7</sup> and current diamond-anvil techniques can achieve much greater pressures, the present work that extends the pressure range studied to 400 GPa

should provide a guide to future experiments.

Searches for candidate high-pressure structures of  $\text{YH}_3$  were performed using an evolutionary algorithm<sup>17,18</sup> method developed for crystal-structure prediction. This was combined with structural optimizations using the Vienna *ab initio* simulation (VASP) code<sup>19</sup> and projector-augmented plane-wave (PAW) potentials.<sup>20</sup> The Y and H potentials employed  $4s4p5s4d$  (11 electrons) and  $1s$  as valence states, respectively, with the Perdew-Burke-Ernzerhof (PBE) exchange-correlation functional.<sup>21</sup> A high energy cutoff of 910 eV was used. The searches using an evolutionary algorithm were performed at different pressures up to 300 GPa, and were limited to the primitive cells with 2 and 3  $\text{YH}_3$  formula units. The enthalpy,  $E+PV$ , was calculated at 0 K, where  $E$  is the static crystal energy,  $P$  the pressure, and  $V$  the volume. This was calculated for the energetically most favorable structures selected from trajectories produced in the evolutionary algorithm procedure. The  $k$ -point meshes<sup>22</sup> for candidate structures were scaled according to the reciprocal-lattice vectors with a basic division of 12. Phonon calculations were performed using the ABINIT program<sup>23</sup> employing the linear-response method, Hartwigsen-Goedecker-Hutter pseudopotentials<sup>24</sup> and the PBE exchange-correlation functional with same valence configurations as the PAW potentials. A  $4 \times 4 \times 4$   $q$ -point mesh was used for Brillouin-zone (BZ) sampling for phonon calculations. At each  $q$  point, the dynamical matrix was calculated with a  $10 \times 10 \times 10$   $k$ -point mesh.

The structural search results are presented in Fig. 1 where the enthalpies of the most energetically competitive structures are compared over the pressure range 0–400 GPa. Structural searches recovered the earlier known high-pressure fcc structure and also revealed additional structures in other pressure ranges. The  $P\bar{3}c1$  structure, identified in recent neutron-diffraction experiments,<sup>14,15</sup> is stable from ambient pressure up to 12 GPa, which is then replaced by a lower-enthalpy  $C2/m$  structure. It should be noted that the other two proposed ambient-pressure structures<sup>12,13</sup> have almost same total energies with the  $P\bar{3}c1$  structure (i.e., within 0.001 eV/ $\text{YH}_3$ ) and a different choice would not affect the predicted phase transition behavior. At 20 GPa, the optimized structural parameters for the  $C2/m$  structure are: Y1:

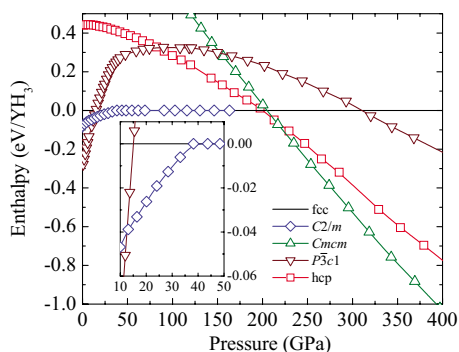


FIG. 1. (Color online) Calculated enthalpies as functions of pressure for  $\text{YH}_3$  predicting successive phase transitions to the following structures,  $P\bar{3}c1$ ,  $C2/m$ , fcc, hcp, and  $Cmcm$ . The enthalpy for the fcc phase is taken as the reference enthalpy.

$4i$  0.3333, 0, 0.206;  $Y2$ :  $2c$  0, 0, 0.5;  $H1$ :  $8j$  0.1676, 0.2491, 0.2739;  $H2$ :  $4i$  0.3317, 0.5, 0.2701,  $H3$ :  $2d$  0, 0.5, 0.5,  $H4$ :  $4g$  0, 0.2425, 0 with  $a=11.133$ ,  $b=4.632$ ,  $c=3.636$  Å, and  $\beta=72.83^\circ$ . The  $C2/m$  structure is a distorted form (via a Peierls distortion,<sup>25</sup> see later) of fcc and the magnitude of distortion decreases with increasing pressure. At 38 GPa, the  $C2/m$  structure completely transforms to fcc. The stable range for the  $C2/m$  structure, is reasonably comparable with the stable range for the intermediate phase connecting the ambient-pressure phase and fcc (9–24 GPa), indicating that the  $C2/m$  structure is a candidate model for the intermediate phase. The fcc structure is a stable phase over a large pressure range up to 200 GPa, at which pressure the predicted hcp structure (space group  $P6_3/mmc$ ) becomes more stable. At 205 GPa, the optimized structural parameters for the hcp structure are:  $Y$ :  $2c$  0.6667, 0.3333, 0.75;  $H1$ :  $4f$  0.6667, 0.3333, 0.4161;  $H2$ :  $2a$  0, 0, 0 with  $a=2.773$  and  $c=5.315$  Å. It is interesting that the hcp structure enters the phase diagram at such a high pressure. The  $P\bar{3}c1$  structure, as a Peierls distorted form of hcp,<sup>26</sup> however enters the phase diagram at ambient pressure. The hcp structure is only predicted to be stable in a narrow pressure range to 214 GPa, where a  $Cmcm$  structure becomes the stable phase and remains stable to at least 400 GPa—the highest pressure in the present study. At 250 GPa, the optimized structural parameters for the  $Cmcm$  structure are:  $Y$ :  $4c$  0, 0.1202, 0.75;  $H1$ :  $8f$  0, 0.3956, 0.9169;  $H2$ :  $4c$  0, 0.1796, 0.25 with  $a=2.613$ ,  $b=6.036$ , and  $c=4.136$  Å. The  $Cmcm$  structure is another distorted form originating from hcp. The distortion is analogous to a Burgers deformation<sup>27</sup> consisting of strains within the hexagonal planes and shear between the neighboring planes. The high-pressure phase transitions of  $\text{YH}_3$  are seen to be strongly associated with distortions from simple basic structures. Two consecutive Peierls distortions from hcp and fcc structures, respectively, result into two stable phases  $P\bar{3}c1$  and  $C2/m$  structures below 38 GPa. At higher pressure, the fcc and hcp structures become more favored than distorted forms up to 214 GPa. Upon increasing the pressure further, a Burgers deformation becomes more favored in hcp and results in a stable  $Cmcm$  structure.

The  $C2/m$  structure originates from distorting a fcc lattice by atomic translations and deformation of the fcc unit cell.

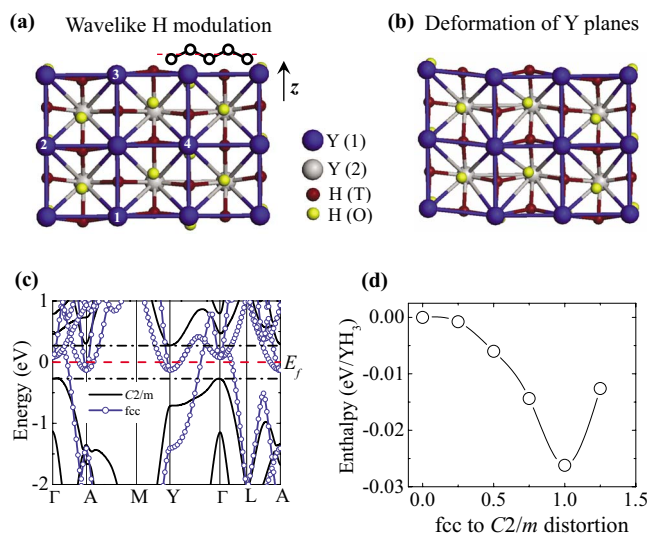


FIG. 2. (Color online) The Peierls distortion in fcc structure and the resulting  $C2/m$  structure at 20 GPa. The distortion includes (a) the wavelike modulation of H atoms and the (b) deformation of Y framework. The dark and light Y atoms represent atoms in adjacent layers. The dark and light H atoms represent atoms in tetrahedral (T) and octahedral (O) sites, respectively. The numbers 1–4 outline the original fcc unit cell. (c) Comparison of the band structures of  $C2/m$  and fcc phases in the  $C2/m$  Brillouin zone. The dashed and dashed-dotted lines indicate the Fermi level and energy gaps in the fcc and  $C2/m$  structures, respectively. (d) The calculated enthalpy of the  $C2/m$  structures as a function of distortion (see text). The enthalpy for the fcc phase is taken as a reference.

The  $C2/m$  cell is defined by the basic vectors  $(0, -1, -2)$ ,  $(1, 0, 0)$ ,  $(0, 0.5, -0.5)$  in terms of the conventional orthogonal fcc lattice vectors with only slight modifications in the lattice constants ( $<6\%$  at 20 GPa). The atomic translations involve two basic components, the wavelike modulation of H atoms [Fig. 2(a)] and the deformation of Y framework [Fig. 2(b)]. Figure 2(a) shows the geometry of the H distortions toward the  $C2/m$  structure at 20 GPa while keeping the Y framework unchanged. It is seen that some H atoms move out of the plane formed by the metallic Y atoms and are displaced symmetrically or asymmetrically. This distortion is identified as a Peierls distortion, which results in a vertical modulation ( $z$  axis) of H positions with a horizontally propagating wave vector ( $xy$  plane). For the H atoms in octahedral sites,  $1/3$  of them stay in the Y plane,  $1/3$  of them move above the Y plane by  $0.1c$ , and the other  $1/3$  move down by the same distance. This atomic modulation reduces the fcc symmetry to that of  $C2/m$  with the H atoms in octahedral sites remaining in or moving out the Y planes to form new  $2d$  and  $4i$  symmetry sites, respectively. The H atoms in tetrahedral sites are modulated in the same pattern with a smaller magnitude of displacement,  $0.06c$ . The new symmetry sites are  $4g$  and  $8j$  for H atoms in tetrahedral sites remaining in and moving out the Y planes, respectively. To accommodate the H modulation, the Y framework also goes through a similar wavelike modulation with a shifting of  $0.04c$  and breaks the Y positions into  $2c$  and  $4i$  symmetry sites [Fig. 2(b)]. Notably, previous studies identified the same type of Peierls distortion in the  $P\bar{3}c1$  structure and attributed the insulating behavior to the wavelike modulation of H atoms.<sup>26</sup>

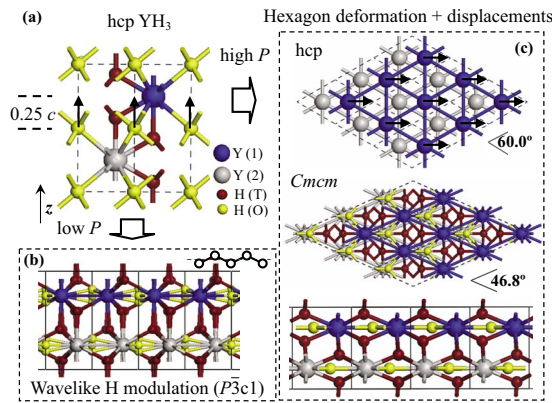


FIG. 3. (Color online) The pressure-dependent distortions from the hcp structure. Both distortions are initialized by moving the H atoms in octahedral sites from the hcp lattice (a) toward the metallic Y(1) plane. The arrows indicate displacements of the H atoms in octahedral sites. (b) The wavelike modulation of H atoms in octahedral sites at low pressure. (c) The deformation of hexagonal planes and the relative displacements of neighboring planes at high pressure. The arrows indicate the displacement direction of planes.

In Fig. 2(c), the band structure of  $C2/m$  structure is compared with that of fcc at 20 GPa. The bands close to the Fermi level are strongly affected by the distortion, and an indirect energy gap is opened up between the  $\Gamma$  and Y points in the BZ. The  $C2/m$  structure, therefore, is insulating with a calculated band gap of 0.54 eV at 20 GPa. The basic principles for this type of metal-insulator transition are rather general. The initial periodic lattice of fcc acquires a periodic modulation of atoms, which acts as an additional periodic potential for the electrons. If the wave vector of the atomic modulation is comparable to the Fermi momentum, an energy gap will be opened, with the conduction and valence-band energies nearby the Fermi level being raised and lowered [Fig. 2(c)]. The lowering of valence bands will also reduce the static crystal energy and stabilize the  $C2/m$  structure. In order to demonstrate this, the enthalpy as a function of distortion is calculated using fcc as a starting structure [Fig. 2(d)]. Along the transition pathway, the 0.0 and 1.0 distortion corresponds to the fcc and  $C2/m$  structures, respectively. It is clear that the enthalpy of the fcc (undistorted) is at local maximum and the  $C2/m$  structure (fully distorted) occupies local minimum. With increasing pressure, the distortion decreases and this results in a narrowing of the band gap. Once the  $C2/m$  structure completely changes to fcc at 38 GPa, the band gap closes completely and  $\text{YH}_3$  becomes metallic. The pressure-dependent insulating properties of the  $C2/m$  structure agree well with the experimental observation<sup>4-7</sup> for the intermediate phase in this pressure range.

The high-pressure  $Cmcm$  structure originates from distorting the hcp lattice and is closely related to the appearance of the low-pressure  $P\bar{3}c1$  structure. Both  $Cmcm$  and  $P\bar{3}c1$  structures are initialized by moving the H atoms in octahedral sites in hcp by  $0.25c$  toward the Y plane [Fig. 3(a)]. The hexagonal  $\text{YH}_3$  structure then is stabilized by these unconventional H movements, which yield stronger H-Y interactions and result in a considerable drop of band energies.<sup>26</sup> To

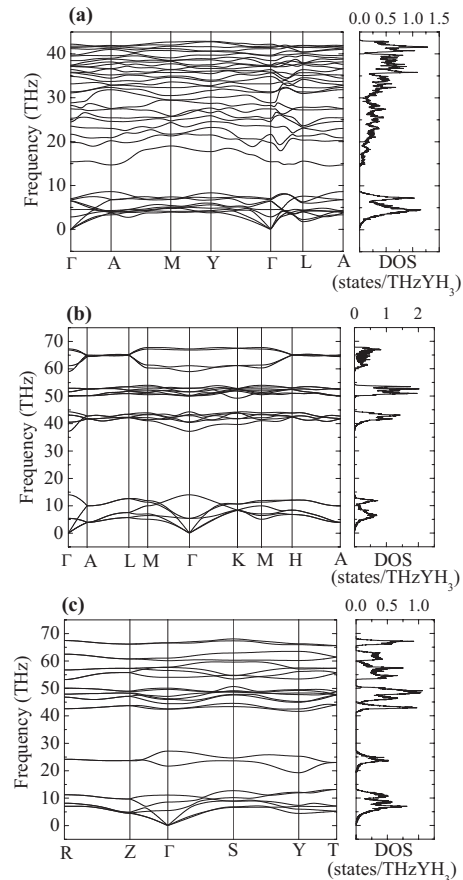


FIG. 4. Phonon band structures and DOS for (a)  $C2/m$ , (b) hcp, and (c)  $Cmcm$  structures of  $\text{YH}_3$ , calculated at 20, 200, and 225 GPa, respectively.

accommodate the additional potential induced by these movements, the H atoms in tetrahedral sites also experience slight vertical shifting ( $z$  axis) and horizontal rotations ( $xy$  plane). The next (final) step of distortion is pressure dependent, and results in the  $P\bar{3}c1$  and  $Cmcm$  structures at different pressures. At low pressure, the H atoms in octahedral sites (now in the plane of Y atoms) have additional shifts off high-symmetry sites and form the wavelike modulation, resulting in the  $P\bar{3}c1$  structure [Fig. 3(b)]. This type of H displacement is identical to the Peierls distortion identified in the  $C2/m$  structure and is responsible for the unusual electronic properties of the  $P\bar{3}c1$  structure.<sup>26</sup> At high pressure, the H atoms in octahedral sites remain located in the planes of Y atoms. The planes go through a tensile deformation  $e_{xx}-e_{yy}$  and change the two central angles in (110) planes from  $60^\circ$  to  $46.8^\circ$  [Fig. 3(c)], which lowers the hcp symmetry to orthorhombic  $Cmcm$ . Simultaneously, the neighboring planes move against each other by  $0.42$  [ $110$ ], which converts the  $Y 2c$  symmetry sites in hcp into the  $4c$  sites in the  $Cmcm$  structure [Fig. 3(c)]. This distortion is similar to a Burgers transformation, which was originally proposed to describe the hcp  $\rightarrow$  bcc transition through a common subgroup  $Cmcm$ .<sup>27</sup> The H atoms in octahedral sites move within the planes of Y atoms and occupy another group of  $4c$  symmetry sites. The H atoms in tetrahedral sites, while having

slight distortion off these sites, occupy  $8f$  symmetry sites. The band structure calculation indicates that the  $Cmcm$  structure is a weak metal, with a small density of states (DOS) at the Fermi level, e.g., only 0.2 per  $YH_3/eV^{-1}$  at 220 GPa. It is interesting to note that at high pressure in the  $Cmcm$  structure, the H atoms are not displaced out of the plane of Y atoms with the result that H atoms do not form close pairs. This is in contrast to proposals<sup>28,29</sup> derived from studies on several other hydrides.

The stabilities of the three predicted  $YH_3$  structures, the  $C2/m$ , hcp, and  $Cmcm$ , were established from the phonon calculations [Figs. 4(a)–4(c)]. The absence of imaginary frequencies confirms that the three structures are stable and therefore should be observable. The occurrence of optic modes in the 21–27 THz frequency region in the  $Cmcm$  structure originates primarily from H-atom vibrations out of the planes of Y atoms. Recently it was predicted that the fcc

$YH_3$  could be a good superconductor.<sup>16</sup> Thus, it is interesting to investigate whether the hcp and  $Cmcm$  metallic phases are superconducting as well. Using the highest phonon frequency as a measure, the estimated Debye temperature for the  $Cmcm$  structure is about 3400 K at 225 GPa. Such a high Debye temperature is promising for enhanced superconductivity behavior; however, the very low DOS at the Fermi level will strongly limit its occurrence. The coexistence of high Debye temperature and low DOS at the Fermi level has been, for example, seen before in high-pressure  $AlH_3$ , and the competition between these features results in a nonsuperconducting phase, at least down to 4 K.<sup>30</sup> In this respect, the question of whether the hcp and  $Cmcm$  structures are superconducting can only be answered by the experiments. The present results encourage further experimental study of  $YH_3$  at high pressure.

- <sup>1</sup>J. N. Huiberts, R. Griessen, J. H. Rector, R. J. Wijngaarden, J. P. Dekker, D. G. de Groot, and N. J. Koeman, *Nature (London)* **380**, 231 (1996).
- <sup>2</sup>R. J. Wijngaarden, J. N. Huiberts, D. G. Nagengast, J. H. Rector, R. Griessen, M. Hanfland, and F. Zontone, *J. Alloys Compd.* **308**, 44 (2000).
- <sup>3</sup>A. Ohmura, A. Machida, T. Watanuki, K. Aoki, S. Nakano, and K. Takemura, *Phys. Rev. B* **73**, 104105 (2006).
- <sup>4</sup>T. Palasyuk and M. Tkacz, *Solid State Commun.* **133**, 477 (2005).
- <sup>5</sup>A. Machida, A. Ohmura, T. Watanuki, T. Ikeda, K. Aoki, S. Nakano, and K. Takemura, *Solid State Commun.* **138**, 436 (2006).
- <sup>6</sup>T. Kume, H. Ohura, S. Sasaki, H. Shimizu, A. Ohmura, A. Machida, T. Watanuki, K. Aoki, and K. Takemura, *Phys. Rev. B* **76**, 024107 (2007).
- <sup>7</sup>A. Machida, A. Ohmura, T. Watanuki, K. Aoki, and K. Takemura, *Phys. Rev. B* **76**, 052101 (2007).
- <sup>8</sup>J. S. de Almeida, D. Y. Kim, C. Ortiz, M. Klintonberg, and R. Ahuja, *Appl. Phys. Lett.* **94**, 251913 (2009).
- <sup>9</sup>N. F. Miron, V. I. Shcherbak, V. N. Bykov, and V. A. Levdkin, *Kristallografiya* **17**, 404 (1972) [*Sov. Phys. Crystallogr.* **17**, 342 (1972)].
- <sup>10</sup>A. Pebler and W. E. Wallace, *J. Phys. Chem.* **66**, 148 (1962).
- <sup>11</sup>T. J. Udovic, Q. Huang, R. W. Erwin, B. Hjörvarsson, and R. C. Ward, *Phys. Rev. B* **61**, 12701 (2000).
- <sup>12</sup>P. van Gelderen, P. J. Kelly, and G. Brocks, *Phys. Rev. B* **63**, 100301(R) (2001).
- <sup>13</sup>W. Wolf and P. Herzig, *Phys. Rev. B* **66**, 224112 (2002).
- <sup>14</sup>V. K. Fedotov, V. E. Antonov, I. O. Bashkin, T. Hansen, and I. Natkaniec, *J. Phys.: Condens. Matter* **18**, 1593 (2006).
- <sup>15</sup>T. J. Udovic, Q. Huang, A. Santoro, and J. J. Rush, *Z. Kristallogr.* **223**, 697 (2008).
- <sup>16</sup>D. Y. Kim, R. H. Scheicher, and R. Ahuja, *Phys. Rev. Lett.* **103**, 077002 (2009).
- <sup>17</sup>A. R. Oganov and C. W. Glass, *J. Chem. Phys.* **124**, 244704 (2006).
- <sup>18</sup>Y. Yao, J. S. Tse, and K. Tanaka, *Phys. Rev. B* **77**, 052103 (2008).
- <sup>19</sup>G. Kresse and J. Hafner, *Phys. Rev. B* **47**, 558 (1993).
- <sup>20</sup>G. Kresse and D. Joubert, *Phys. Rev. B* **59**, 1758 (1999).
- <sup>21</sup>J. P. Perdew, K. Burke, and M. Ernzerhof, *Phys. Rev. Lett.* **77**, 3865 (1996).
- <sup>22</sup>H. J. Monkhorst and J. D. Pack, *Phys. Rev. B* **13**, 5188 (1976).
- <sup>23</sup>X. Gonze, J. M. Beuken, R. Caracas, F. Detraux, M. Fuchs, G. M. Rignanese, L. Sindic, M. Verstraete, G. Zerah, F. Jollet, M. Torrent, A. Roy, M. Mikami, Ph. Ghosez, J.-Y. Raty, and D. C. Allan, *Comput. Mater. Sci.* **25**, 478 (2002).
- <sup>24</sup>M. Krack, *Theor. Chem. Acc.* **114**, 145 (2005).
- <sup>25</sup>R. E. Peierls, *Quantum Theory of Solids* (Clarendon Press, Oxford, 1955).
- <sup>26</sup>Y. Wang and M. Y. Chou, *Phys. Rev. Lett.* **71**, 1226 (1993).
- <sup>27</sup>W. G. Burgers, *Physica (Amsterdam)* **1**, 561 (1934).
- <sup>28</sup>J. S. Tse, Y. Yao, and K. Tanaka, *Phys. Rev. Lett.* **98**, 117004 (2007).
- <sup>29</sup>Y. Yao, J. S. Tse, Y. Ma, and K. Tanaka, *EPL* **78**, 37003 (2007).
- <sup>30</sup>I. Goncharenko, M. I. Erements, M. Hanfland, J. S. Tse, M. Amboage, Y. Yao, and I. A. Trojan, *Phys. Rev. Lett.* **100**, 045504 (2008).